X-551-69-137
PREPRINT

NASA TM X-63572

A REVIEW OF GODDARD RANGE AND RANGE RATE SYSTEM MEASUREMENTS AND DATA PROCESSING TECHNIQUES

T. J. GRENCHIK
B. H. PUTNEY

APRIL 1969

GSFC — GODDARD SPACE FLIGHT CENTER
GREENBELT, MARYLAND

FACILITY FORM 602

N69-29748 (ACCESSION NUMBER)	(THRU) 1
42 (PAGES)	(CODE)
TMX-63572 (NASA CR OR TMX OR AD NUMBER)	30 (CATEGORY)

X-551-69-137
PREPRINT

A REVIEW OF GODDARD RANGE AND RANGE RATE SYSTEM MEASUREMENTS AND DATA PROCESSING TECHNIQUES

T. J. Grenchik
B. H. Putney

April 1969

GODDARD SPACE FLIGHT CENTER
Greenbelt, Maryland

ABSTRACT

The methods involved in satellite tracking data gathering and the procedures followed in satellite orbit determination from the tracking data are necessarily of interest both to the tracking systems engineer and the orbit analyst. It is the purpose of this paper to document for such interests a description of the Goddard Range and Range Rate system's measurements, limitations of these measurements, and effects of partial processing of the measurement data prior to final orbit computation. The description of measurement of satellite radial velocity, i.e. range rate, is given special attention since much controversy arises over its definition, measurement, and usage in orbit determination.

CONTENTS

A REVIEW OF GODDARD RANGE AND RANGE RATE SYSTEM MEASUREMENTS AND DATA PROCESSING TECHNIQUES

T. J. Grenchik
B. H. Putney
Goddard Space Flight Center

1.0 INTRODUCTION

Many of the shortcomings of orbit determination result from the separation and semi-independent operation of each of many specialists responsible for a portion of the overall orbit determination process. The separations may be classified loosely as tracking system designer, tracking system operator, tracking system engineer (monitor), data preprocessor (data compressor), and orbit analyst. The bridging and interchange of information between these disciplines would be the ideal means of error reduction in orbit determination and prediction.

In this report the data preprocessing and the basic tracking system operation are described in simple terms for both the Goddard Range and Range Rate (GRARR) System and the Applications Technology Range and Range Rate System, an outgrowth of GRARR. In both systems the primary measurements are radial range and rate of change of radial range. In this report all significant system error sources are described and/or referenced. Additional tutorial references are included for those interested. Time-tagging errors are given the greatest attention because it is felt that this class of errors is one of the simplest to remove in the tracking data preprocessing (data editing and/or compression). Some representative values of time-tag errors are used to demonstrate their influence in orbit determination.

In the time-tag error class, the uncertainty in WWV transmission time from the Colorado or Hawaii transmission sites to any STADAN tracking site is the dominant source of error for the range rate measurement. The uncertainty in the time of the reception at the station is approximately 1 millisecond. If a constant radial acceleration of 400 m/sec^2 (worst case assumption) coincided with this uncertainty in time tag, a range rate error of approximately 40 cm/sec would result. It is estimated that equipment delays account for range rate time-tag errors of only 200 microseconds.

In the range measurement, if a constant spacecraft radial velocity of 10^4 m/sec (worst case) is assumed to coincide with the 1 millisecond WWV uncertainty, a range error of 10 meters would result. For the range time tagging, there may be equipment time delay errors which are greater than 1 millisecond. In one specific case an error of 2 milliseconds was attributed to equipment delays. Here, additional field measurement and laboratory simulation is called for to verify or disprove this magnitude of equipment delay.

The range rate measurement has been described in more detail than the range measurement to emphasize its nature as an average measurement of range rate over a relatively long time interval. The range measurement can be categorized as an instantaneous measurement and does not require an averaging correction such as applied to the range rate measurement.

Error sources such as speed of light uncertainties, ionospheric and tropospheric effects have not been considered in this report because they are beyond the specialities of the authors.

1.1 PREVIOUS ANALYSES

Many documents concerning Goddard Range and Range Rate (GRARR) System operation have been published. This paper repeats only that information presented previously which is necessary for the reader's overall grasp of system operation beginning with the recorded tracking data and ending just prior to orbit computation. In those sections dealing with processing of the GRARR measurement data for orbit computation little of what is included herein has been published previously. This documentation of the data handling then, will aid the tracking system engineer in comprehending the importance of the various classes of errors in the orbit computation.

1.2 TYPES OF GRARR MEASUREMENTS

The Goddard Range and Range Rate System, as the name implies, measures range and the rate of change of range between the ground tracking station and spacecraft. These measurements are taken periodically (generally once per second) and labelled with the time of occurrence of each measurement. Hence they are time samples of the range and range rate. Along with the primary measurements of range and range rate, samples of antenna pointing angle are also taken although at present they are not generally used in orbit computation. A detailed description of the Goddard Range and Range Rate System, its conception, evolution, and performance is available in Reference 1, but sufficient explanation of the measurements will be given in appropriate sections of this report for reader comprehension without delving into system detail.

2.0 THE RANGE RATE MEASUREMENT

The range rate measurement is a measure of the apparent frequency shift of the ground and spacecraft transmitter frequency caused by the relative motion between the spacecraft and the tracking station. One may argue whether the Doppler effect is better described as an apparent shift in frequency or apparent shift in phase angle of the electromagnetic radiation. No difficulty arises from either consideration since phase and frequency are linearly related by:

$$\frac{d\phi}{dt} = \omega \qquad (1).$$

where ϕ is phase angle in radians and ω is radian frequency. Dr. Kruger formerly of Goddard Space Flight Center (GSFC) in Reference 6 amply treats the subject of Doppler frequency shift including relativistic effects. Here the subject is treated more simply but the same results are attained.

2.1 RANGE RATE AVERAGING ERRORS

The most important point, which cannot be stressed too strongly, is that the measurement of the frequency shift requires a finite amount of time. In fact longer times are preferable since generally the frequency measure becomes better with the length of the phase count measurement. Of course, what must be considered with the longer measurement is any change in range rate during the measurement interval masked by the averaging effect.

In the Goddard Range and Range Rate (GRARR) system, the average Doppler frequency, $\bar{f}_d$, is established by measuring the time interval required to count a predetermined number of cycles of the instantaneous Doppler frequency plus a fixed bias frequency. A bias frequency is summed with the Doppler frequency in order to sense the direction of the range rate in a simple manner. In the GRARR system δ_{RR} is measured where

$$\delta_{RR} = \frac{N}{f_b + \bar{f}_d} \tag{2}$$

and δ_{RR} is the time interval in seconds required for counting a fixed number (N) of cycles of bias frequency plus Doppler frequency $(f_b + \bar{f}_d)$. δ_{RR} is measured by means of a time interval counter which counts the number of cycles of a reference frequency occurring during the time interval δ_{RR} corresponding to N cycles of $f_b + \bar{f}_d$. The readout of the time interval counter, C_0, at the end of the measurement is related to δ_{RR} by:

$$C_0 = f_r \, \delta_{RR} \tag{3}$$

where C_0 is the count of the time interval counter in cycles and f_r is the reference frequency counted in cycles per second. N and the sample rate* are chosen such that δ_{RR} is between one half and one second.

To estimate the change in instantaneous radial velocity that can occur during a one second interval, it is required to look at the second and higher order derivatives of radial range (d^2R/dt^2, d^3R/dt^3, etc.) under some assumed worse case conditions. In Reference 2, Section V, an elliptical orbit with an apogee of 60,000 nautical miles and a perigee of 150 nautical miles is assumed. At perigee the rate of change of radial velocity d^2R/dt^2 can be a maximum of 435 m/sec² with reference to a ground station almost underneath the point of perigee. Over a one second interval, if d^2R/dt^2 were constant at 435 m/sec² the radial velocity dR/dt would change 435 m/sec.

*Sample rate can be set at other than a one per second rate. See Reference 3.

For example, the counting of Doppler frequency (plus bias frequency) over a one second measurement interval centered at perigee would give an average Doppler frequency of approximately zero cycles. The sign of the Doppler would be one polarity during the first half-second approaching perigee and change to the opposite polarity while receding from perigee. The average Doppler frequency, while correct, masks the instantaneous change in Doppler frequency. If the Doppler measurement were not made with the time interval centered at perigee, it is obvious how large differences between the instantaneous Doppler and the averaged Doppler (represented by the count, C_0) would occur. Dr. Kruger in Reference 7 explores averaging errors for low circular orbits and suggests corrections to be made for all types of orbits. This correction requires estimates of higher order time derivatives of range available from nominal orbit predictions. This correction technique will be discussed in greater detail under the data handling section of this report.

It should be noted that the value of d^2R/dt^2 is a critical function of orbit geometry. For example, at the 60,000 nautical mile apogee of the previously assumed orbit, d^2R/dt^2 is $-1.85(10^{-2})$ m/sec^2 (minimum value) so that a range rate change over a one second time interval in this case would amount to approximately 2 cm/sec. For the case of constant spacecraft radial velocity with respect to a ground station (approximated during certain trajectories) the length of the time interval during the Doppler plus bias measurement would have no effect on the computation of instantaneous Doppler frequency.

2.2 BASIC ELECTRONIC SCHEME AND THE DOPPLER EQUATION

In Equation 2, $\bar{f}_d$ was defined as the average Doppler frequency without demonstrating its relationship to spacecraft average range rate.* In this section the relationship will be derived. Figure 1 shows the Doppler extraction process as it occurs in the Motorola built GRARR system. A more detailed description is presented in Reference 2. This basic example is suitable for explanation of all GRARR system Doppler extraction processes.

In the lower left hand corner of Figure 1 an oscillator of frequency f_t/M is multiplied by M to arrive at a ground transmitter frequency of f_t. At the spacecraft transponder an apparent frequency of Kf_t is received because of the spacecraft motion relative to the ground transmitter. From classical physics the multiplier K for a fixed source and a moving observer (spacecraft) is given by:

$$K = \frac{c - \frac{dR}{dt}}{c} \tag{4}$$

where K is a time varying dimensionless scalar, c is the speed of light in m/sec, and dR/dt is the instantaneous range rate of the spacecraft in m/sec. In Figure 1, v and dR/dt are used interchangeably. The apparent frequency will be greater than the transmitted frequency, f_t, under the conditions

*In preceding paragraphs the measurements are termed radial range and radial velocity. Common usage also ascribes the simpler names range and range rate.

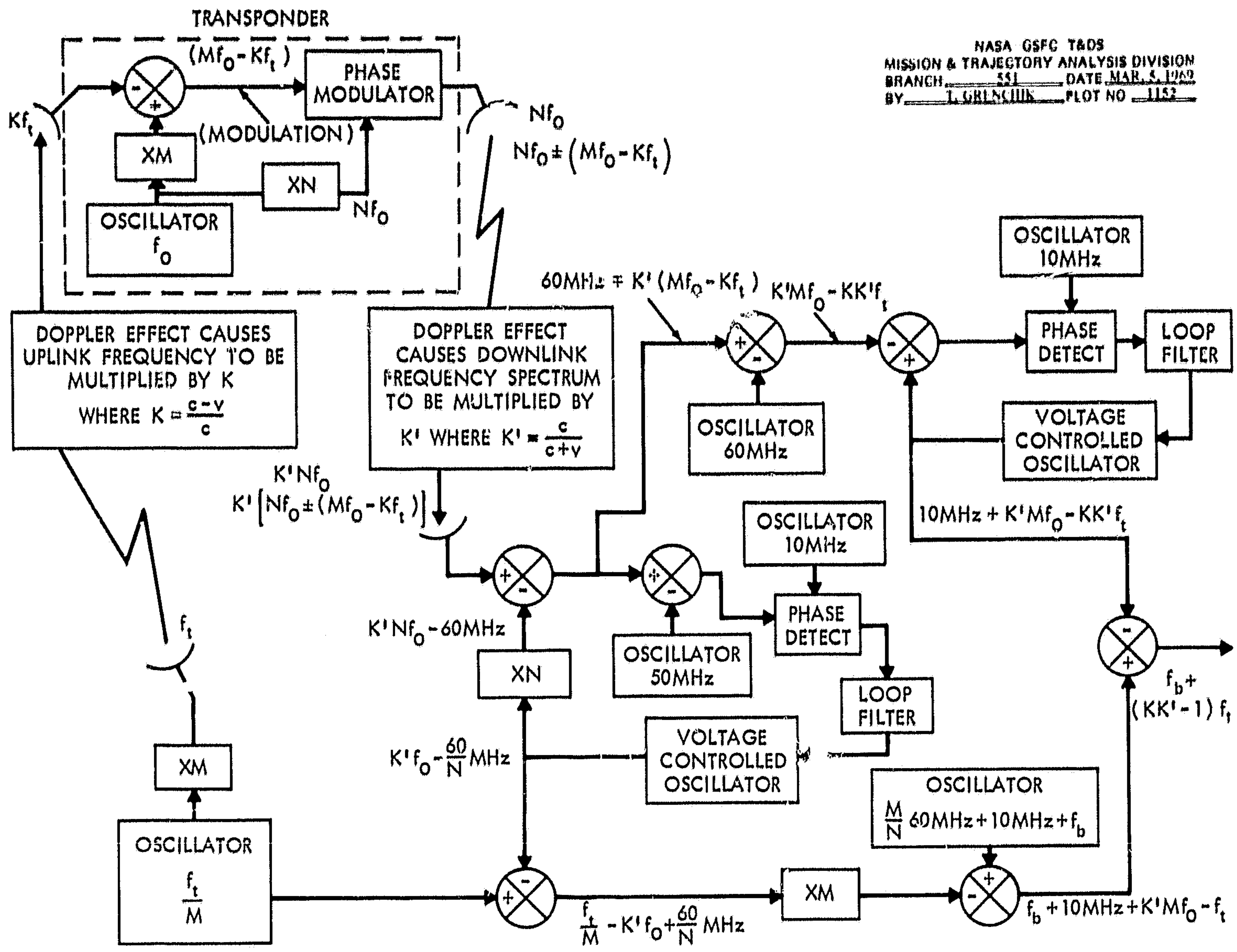

Figure 1—Doppler frequency extraction process.

of decreasing separation (decreasing range and hence decreasing range rate). This apparent change in frequency is analogous to the higher pitched tone heard from the locomotive diesel horn upon approach and the lower pitched tone upon recession. This physical property implies that dR/dt is negative for approach and $K = (c - dR/dt)/c > 1$ under these conditions.

Upon reception at the spacecraft, the frequency Kf_t is mixed to a lower frequency $Mf_0 - Kf_t$ and subsequently is used to vary the phase of the spacecraft transmitted frequency Nf_0. Nf_0 is derived from the spacecraft oscillator f_0 and the spacecraft frequency multiplier N. Thus, in the spacecraft transmitted output, a downlink frequency Nf_0 is modulated by a frequency, $Mf_0 - Kf_t$, which contains the Doppler information on the uplink frequency f_t.

Fourier analysis of the spacecraft downlink transmission enables the separation of the modulated signal into three significant frequency components:

$$Nf_0 \quad \text{(carrier frequency)}$$

$$Nf_0 - Mf_0 + Kf_t \quad \text{(lower sideband)}$$

$$Nf_0 + Mf_0 - Kf_t \quad \text{(upper sideband)}$$

These are shown at the transponder antenna in Figure 1. Each of these components upon reception at the ground appears to be multiplied by K' because of the relative motion of spacecraft and ground station. K' is defined as

$$K' = \frac{c}{c + \frac{dR}{dt}} \tag{5}$$

where K' is a time varying dimensionless scalar, c is the speed of light in m/sec and dR/dt is the instantaneous range rate of the spacecraft in m/sec as defined previously. The derivation of K' follows from the frequency change apparent to a fixed observer (ground station) from a moving transmitter (spacecraft). Recall that an apparent increase of frequency comes about from a diminishing separation. dR/dt must be negative under these conditions and $K' = c/(c+v) > 1$.

In the ground receiver in Figure 1, the carrier term $K' Nf_0$ along with a 60 MHz term which sets the 1st IF frequency is reconstructed by the Voltage Controlled Oscillator and the times N multiplier. The upper and lower sideband frequencies $K'\left[Nf_0 \pm (Mf_0 - Kf_t)\right]$ are filtered off by the loop filter. Before filtering the upper and lower sidebands (now at the 60 MHz IF) are sent to a 60 MHz mixer which removes the 60 MHz term, leaving only a frequency term $K' Mf_0 - KK' f_t$. This frequency term along with a 10 MHz term are reconstructed by the 2nd voltage controlled oscillator.

The ground transmitter oscillator f_t/M is mixed with the reconstructed downlink carrier term $K' f_0 - 60/N$ MHz, the resulting frequency is multiplied by M, a bias frequency f_b is applied in the next mixer and finally in the last mixer, all frequency terms are removed except $f_b + (KK' - 1) f_t$. The spacecraft oscillator terms (f_0) have been removed and the resulting expression $(KK' - 1) f_t$ when converted in terms of dR/dt equals

$$f_d = - \frac{\frac{dR}{dt}(t) + \frac{dR}{dt}\left(t + \frac{R}{c}\right)}{c + \frac{dR}{dt}\left(t + \frac{R}{c}\right)} f_t . \tag{6}$$

The time difference of R/c occurs because K affects the uplink at one instant and K' affects the downlink at time R/c later. This indicated quantity, f_d, is a time varying function which is averaged by the measurement system over a time δ_{RR}. The average value of f_d over the time δ_{RR} becomes approximately,

$$\bar{f}_d \approx \frac{-2\frac{\Delta R}{\Delta t}}{c + \frac{\Delta R}{\Delta t}} f_t . \tag{7}$$

In review K, K', and dR/dt were defined in terms of a decreasing range causing an increase in frequency, with dR/dt defined as negative under these conditions. By definition R decreases as the spacecraft approaches the ground station. dR/dt must agree in sign convention with R, and is negative for spacecraft approach. The quantity:

$$(KK' - 1) \approx \frac{-2\frac{\Delta R}{\Delta t}}{c + \frac{\Delta R}{\Delta t}} \tag{8}$$

is greater than one and the Doppler frequency is greater than zero, the physical result expected from the Doppler effect. Combining Equations 7, 8, and 2, one obtains:

$$\delta_{RR} \approx \frac{N}{f_b + \frac{-2\frac{\Delta R}{\Delta t}}{c + \frac{\Delta R}{\Delta t}} f_t} \tag{9}$$

In terms of the readout of the GRARR system range rate time interval counter (C_0 in Equation 3), Equation 9 becomes:

$$C_0 \approx \frac{Nf_r}{f_b + \frac{-2\frac{\Delta R}{\Delta t}}{c + \frac{\Delta R}{\Delta t}} f_t} \tag{10}$$

2.3 TABULATION OF DOPPLER MEASUREMENT ERRORS

References 2, 3, and 4 consider the effects of various errors in the range rate measurement and place magnitudes on these measurement errors. Here the intent is not to set exact quantitative limits on these errors but to catalog the errors according to source. For range rate these three classes are:

1. All sources that cause phase (frequency) errors in the $f_b + f_d$ measurement.

2. All sources that cause time interval measurement errors in C_0.

3. All sources that cause error in identifying the correct time of the sample measurement.

3.0 DISCUSSION OF DOPPLER MEASUREMENT ERRORS

3.1 PHASE ERROR IN DOPPLER PLUS BIAS FREQUENCY

Oscillator Instabilities

In Figure 1, there are shown a large number of oscillators: two voltage controlled oscillators in phase locked loops, a transmitter oscillator and multipliers, a spacecraft oscillator and multipliers, receiver oscillators at 50, 60, and 10 MHz, and a receiver oscillator which places the bias frequency into the processing system. Each of these oscillators contribute phase instability to the extracted frequency $f_b + f_d$ since in each conversion a minute phase instability is transferred from the imperfect oscillator to the Doppler frequency. Magnitudes of errors to be expected from each of these oscillators are listed in References 2, 3, and 4. It suffices here to state that the greatest source of error comes from the voltage controlled oscillators in the phase locked loops. This is a direct result of the requirement for a pulling range of several hundred kilohertz. Phase stability and the frequency change capability of a voltage controlled oscillator are in direct opposition to one another; as one gets better, the other becomes worse.

Axis Crossing Detectors

Axis crossing detectors are used throughout the GRARR system to identify times of zero crossings (phase reference points). If a perfect axis crossing detector could be built, it would sense accurately the occurrence of any input signal's magnitude becoming and passing through zero. (Limitations of real axis crossing detectors will be discussed under Time Interval Measurement Errors.) In system operation the input signal's magnitude has been corrupted by noise so that the true occurrences of zero magnitude have been shifted randomly in time. In some instances under sufficiently strong noise conditions, an occurrence of zero magnitude will be deleted, that is, if one were counting zero crossings of a sine wave to measure frequency, the count would be low by the number of zero crossings suppressed by the noise (actually 1/2 of the zero crossings since frequency equals 1/2 of the number of positive and negative going zero crossings).

The phase (frequency) errors caused by system input noise are irreducible unless improvements can be made in the overall receiving system's noise content, or the spacecraft radiated power can be increased sufficiently to force the system noise into a less competitive position. If this were done similar improvements would be required in the system oscillator instabilities to prevent those sources of error from becoming dominant.

At present all sources of error are approximately balanced. If new mission requirements should impose a large improvement factor in range rate error, all sources of error would require proportionate improvements.

3.2 TIME INTERVAL MEASUREMENT ERRORS

In the preceding sections it was shown that there are a number of sources of error which affect the frequency (phase of the Doppler plus bias frequency $(f_b + f_d)$. In this section those errors affecting the measure of the corrupted $f_b + f_d$ frequency will be discussed.

Once the $f_b + f_d$ frequency has been detected in the axis crossing detector, the "noise-free" resultant is counted in a counter which has a preset count limit, N. At the beginning of the count of N a start reference is generated. At the end of the count of N a stop reference is generated. Between the start and the stop reference a time interval is measured. For emphasis a preceding description is repeated here. This time interval is measured by counting cycles of a fixed reference frequency (f_r) from the beginning of the interval until the end of the interval, δ_{RR}. The number of cycles counted multiplied by the time required for one cycle to occur provides a measure of the time interval needed to count N cycles of $f_b + f_d$, that is if

$$\delta_{RR} = \frac{N}{f_b + f_d} \tag{12}$$

the number of cycles counted (C_0) of the reference frequency would equal

$$C_0 = \delta_{RR} f_r \tag{13}$$

C_0 is the system measurement and it is this measurement which is used in orbit computation. Expressing δ_{RR} in terms of C_0 and f_r, and f_d in terms of dR/dt and c, we have:

$$C_0 \approx \frac{N f_r}{f_b + \dfrac{-2\dfrac{\Delta R}{\Delta t}}{c + \dfrac{\Delta R}{\Delta t}} f_t} \tag{14}$$

Start and Stop Pulse Jitter

A perfect axis crossing detector as described previously recognizes the occurrence of the passage of the input signal through zero magnitude. In reality an axis crossing detector works on the principle of a large amplification of the input signal prior to a low level threshold detection of the amplified signal. Figure 2 illustrates this method of detection. Shifts in the threshold level and especially circuit unbalance in the positive and negative thresholds give the effect of shifting the positive and negative slopes of the reconstructed "noise-free" output. Since the start and stop pulses originate from the 1^{st} and N^{th} cycle of the reconstructed $f_b + f_d$ frequency, the jitter in the reconstruction shows as jitter in the start and stop pulses required for the interval measurements.

Quantizing Error

The time interval measurement measures *complete* cycles of the reference frequency,

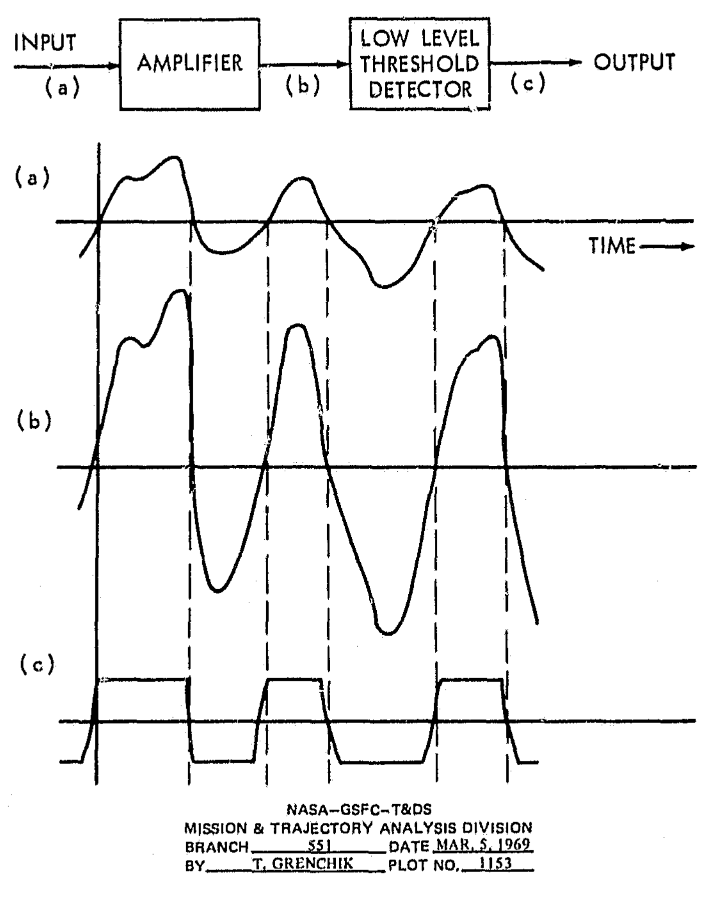

Figure 2—Axis crossing detector operation.

that is if the reference frequency f_r is 10 MHz, the maximum uncertainty in the time interval measurement is related to the time f_r takes to complete a full cycle. The start pulse and the stop pulse are not coherent to the time base frequency f_r so that a maximum error of 0.1μ second can occur at the start pulse and 0.1μ second at the stop pulse.

These quantization errors can be reduced by increasing the frequency of the reference frequency. At present however, the quantization errors are adequately minute. (See References 2, 3, and 4.)

f_r Time Base Reference Short Term Instability

f_r, the 10 MHz reference frequency has an uncertainty associated with its phase (frequency) caused by the minute amounts of noise and spurious signal contained in its generation and amplification. This is evidenced by lengthening or shortening of the cycles of 10 MHz signal which is counted for c_0. Limits on the uncertainty in f_r are set by the mission requirements and the uncertainties generated by other error sources.

3.3 TIME TAGGING ERRORS

In Section 2.1, the averaging affect of the Doppler frequency measurement was noted. In this section similar types of errors will be described, all of which are present if the acceleration and/or higher order derivatives of range are not zero. Figure 3 shows graphically the significant

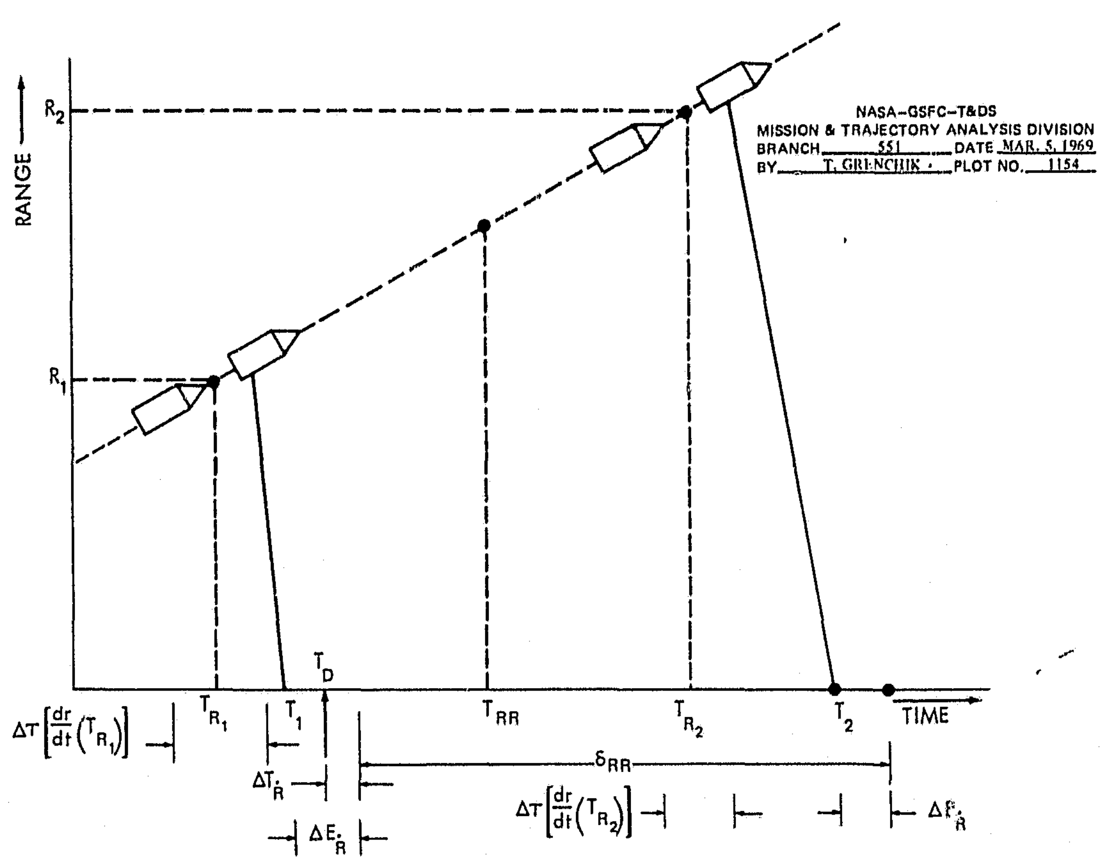

Figure 3—Range rate measurement time tag.

times and time intervals associated with the range rate measurement. Definitions are as follows:

T_{R_1} - Time associated with range R_1

R_1 - Range at T_{R_1}

$\Delta\tau\left[dR/dt\left(T_{R_1}\right)\right]$ - Spacecraft transponder delay at T_{R_1} which is a function of uplink Doppler frequency

T_D - Data time as reported in GRARR format for measurement of range rate

$\Delta T_{\dot{R}}$ - Time interval following T_D, after which range rate measurement actually starts. The reason for this delay will be explained later

T_1 - Time of receipt at ground antenna of first cycle of spacecraft transmission used in Doppler frequency measurement

$\Delta E_{\dot{R}}$ - Time delay from antenna to Doppler extraction process. 1st cycle of spacecraft transmission reaches Doppler extractor at $T_1 + \Delta E_{\dot{R}}$

T_{RR} - Middle of range rate measurement interval (spacecraft time) with which range rate measurement is associated in orbit computation

T_{R_2} - Time associated with range R_2

R_2 - Range at T_{R_2}

$\Delta\tau\left[dR/dt\left(T_{R_2}\right)\right]$ - Spacecraft transponder delay at T_{R_2} which is a function of uplink Doppler frequency

T_2 - Time of receipt at ground antenna of last cycle of spacecraft transmission used in Doppler frequency measurement

δ_{RR} - Time interval measurement of N count of $f_b + f_d$

If T_{RR} is not correctly determined the range rate measurement will have error since the acceleration and higher derivatives of the range are normally present. Some idea of magnitude of these time tagging errors, error in identifying the time T_{RR} absolutely, are of interest.

The times T_1 and T_2 in Figure 3 show the beginning and end points of the range rate counting interval δ_{RR} when referred to reception at the ground antenna. There is a finite time delay, $\Delta E_{\dot{R}}$, in the equipment that extracts $f_b + f_d$, so that the counting process does not begin until $T_1 + \Delta E_{\dot{R}}$, and the counting process does not end until $T_2 + \Delta E_{\dot{R}}$. The time on the ground must be referred to antenna input, actually to the Y-axis of the receiving antenna. (See Reference 8 for the timing reference point of the GRARR receiving system.) Hence, the times of the counting interval referred to the antennas input are T_1 and T_2.

T_D is the reported data time of the measurement but there is a finite time delay $\Delta T_{\dot{R}}$ after T_D before the δ_{RR} measurement begins. This delay is caused by the first cycle of $f_b + f_d$ clearing the N counter before proceeding with the measurement and counting to N + 1 cycles.

In Figure 3, it can be seen that the cycle counting process is actually counting cycles of Doppler frequency which have occurred at the spacecraft prior to reception on the ground. To relate the reception of the frequency at time T_1 to the time of the frequency at the spacecraft, T_{R_1}, we have:

$$T_1 = T_{R_1} + \frac{\Delta\tau}{2}\left[\frac{dR}{dt}\left(T_{R_1}\right)\right] + \frac{R_1}{c} \tag{15}$$

Similarily we find:

$$T_2 = T_{R_2} + \frac{\Delta\tau}{2}\left[\frac{dR}{dt}\left(T_{R_2}\right)\right] + \frac{R_2}{c} \tag{16}$$

The solutions for T_{RR} follows from:

$$T_{RR} = \frac{T_{R_1} + T_{R_2}}{2} \tag{17}$$

$$T_{RR} = \frac{T_1 + T_2}{2} - \frac{1}{4}\left\{\Delta\tau\left[\frac{dR}{dt}\left(T_{R_1}\right)\right] + \Delta\tau\left[\frac{dR}{dt}\left(T_{R_2}\right)\right]\right\} - \frac{1}{2c}\left(R_1 + R_2\right) \tag{18}$$

T_1 and T_2 are related to T_D and δ_{RR} by:

$$T_D = T_1 + \Delta E_{\dot{R}} - \Delta T_{\dot{R}} \tag{19}$$

$$T_2 = T_1 + \delta_{RR} \tag{20}$$

Equation 18 becomes upon elimination of T_1 and T_2

$$T_{RR} = T_D + \Delta T_{\dot{R}} + \frac{\delta_{RR}}{2} - \Delta E_{\dot{R}} - \frac{1}{4}\left\{\Delta\tau\left[\frac{dR}{dt}\left(T_{R_1}\right)\right] + \Delta\tau\left[\frac{dR}{dt}\left(T_{R_2}\right)\right]\right\} - \frac{1}{2c}\left(R_1 + R_2\right) \tag{21}$$

At this point it is also necessary to insert a correction in Equation 21 for synchronization of the ground station time clock to the high frequency (HF) time transmission of WWV and WWVH. (See Reference 11.) For ease of synchronization, the ground station clocks are matched in time to the reception of the transmission and not to the time of the origination of the transmission.* Thus,

*In the near future ground station clocks will be set on time, that is the clocks will include the time delay correction. When this occurs no WWV corrections will be necessary in the GRARR data preprocessing.

for each station, its time clock is "slow" from tens to hundreds of milliseconds, depending on the time delay before reception of the time transmission. The data time T_D used at the ground station is accordingly "slow" and Equation 21 corrected for this slowness is:

$$T_{RR} = T_D + WWV + \Delta T_{\dot{R}} + \frac{\delta_{RR}}{2} - \Delta E_{\dot{R}} - \frac{1}{4}\left\{\Delta\tau\left[\frac{dR}{dt}\left(T_{R_1}\right)\right] + \Delta\tau\left[\frac{dR}{dt}\left(T_{R_2}\right)\right]\right\} - \frac{1}{2c}\left(R_1 + R_2\right) \qquad (22)$$

where WWV is the time delay in seconds from the transmission of the WWV signal to the reception of that signal at the ground station. Each ground station has a measured value for WWV which is an average value of the time delay calculated from many observations. These time delay values are judged to be correct only within one millisecond because of the uncertainties in the height of the ionosphere, tilting of the ionosphere, etc. which cause variation in the mean path length traveled by the transmission.

Recently, an experiment with a portable clock carried aboard the GEOS-B satellite has demonstrated a capability of synchronizing ground stations to within 0.1 millisecond, a factor of ten improvement over the WWV transmission time uncertainty. This improvement was possible because of the precise definition of the GEOS-B orbit and the relatively smaller uncertainties in the time delay of the 136 MHz transmission carrier of the timing signals from the spacecraft to the ground station.

These preliminary descriptions now allow the assignment of magnitude of time tag errors for T_{RR} in Equation 22. WWV can be in error from 0.1 to 1 millisecond. The average value of $\Delta T_{\dot{R}}$ is 50μ seconds for the VHF measurement and 3μ seconds for the S-band measurement. $\Delta E_{\dot{R}}$ is estimated to be 0.2 milliseconds (and will be discussed in detail in following paragraphs). $\Delta\tau$ transponder delay is never larger than 18μ seconds* so that

$$\frac{1}{4}\left\{\Delta\tau\left[\frac{dR}{dt}\left(T_{R_1}\right)\right] + \Delta\tau\left[\frac{dR}{dt}\left(T_{R_2}\right)\right]\right\}$$

is never larger than 9μ seconds.

The term $(R_1 + R_2)/(2c)$ depends on the range to the spacecraft. For tracking a satellite orbiting the moon this term would be approximately 1.25 seconds.

A review of the time tag errors shows that the order of importance of the errors is as follows:

	Maximum Error in Time Tag	Range Rage Error if $d^2R/dt^2 = 435$ m/sec^2
• $\frac{1}{2c}(R_1 + R_2)$, if not considered in data processing	$1,250,000\mu$ sec	543 m/sec

*VHF transponder delay is approximately 17μ seconds, S-band transponder delay is approximately 3μ seconds.

	Maximum Error in Time Tag	Range Rate Error if $d^2 R/dt^2 = 435$ m/sec ^{2}
• WWV, uncertainty	100-1000μ sec	.0435-.435 m/sec
• $\Delta E_{\dot{R}}$, if not considered in data processing	200μ sec	.0870 m/sec
• $\Delta T_{\dot{R}}$, if not considered in data processing	3-50μ sec	.0013-.021 m/sec
• $\frac{1}{4}\left\{\Delta\tau\left[dR/dt\left(T_{R_1}\right)\right] + \Delta\tau\left[dR/dt\left(T_{R_2}\right)\right]\right\}$ if not considered in data processing	9μ sec	.004 m/sec

Consider a time tag error of 200μ seconds such as $\Delta E_{\dot{R}}$. Again it is necessary to refer to the assumed worst case orbit condition with an acceleration, $d^2 R/dt^2$, maximum of 435 m/sec^2. Over a period of 200μ seconds a constant acceleration of 435 meters per second squared would produce a range rate change of 0.087 meters per second, that is if a time tag error of 200μ seconds coincided with a constant spacecraft acceleration of 435 m/sec^2, the velocity measurement would be in error by 0.087 m/sec.

The time tag error of $\Delta E_{\dot{R}}$ is of special interest since next to the uncertainty in the WWV transmission time, it is the most significant possible source of error. Recall that $\Delta E_{\dot{R}}$ is the time delay through the receiving system from the antenna input to the "N" counter input. In reexamination of Figure 1, nothing is shown which could cause significant delay through the system. Admittedly there is a physical separation of several hundred feet between the receive antenna and the "N" counter but this would only account for a time delay on the order of 1/3 of a microsecond. Yet time delays of approximately 200μ seconds have been seen in one specific case described in Reference 9. In Figure 1 the phase locked loops themselves cause little or insignificant delay to the received signal, principally because the selectivity of the loop filter is small and phase change through the loop filter is correspondingly small. (See Reference 10 for description of the phase slope characteristics of phase locked loops.) What is not shown in Figure 1 are the 10 kHz bandpass filters placed ahead of the phase detectors in the phase locked loops so as to limit the noise bandwidth and present a reasonable signal to noise ratio input to the phase detectors. Gardner, et al., in Reference 10, describes the limitations of practical phase detectors which force additional filtering of the phase detector input. It is this additional filtering which introduces considerable delay through the phase locked loop. In any selective network, the phase angle of the input signal varies as a function of the input frequency, and from greater selectivity greater phase variation (delay) results.

Corrections for this delay, if necessary, can only be obtained from measurements made on the phase characteristics of the selective circuit preceding the phase detector input. In the situation described in Reference 9 where a consistent 200 microsecond delay existed in the range rate measurement time, it is certainly possible to presuppose a delay of this magnitude. No measurements to date have been made of any parts of the system delay affecting the range rate measurement but future investigation will be made to assure that this source of error has not become predominant.

Actual corrections made in the data processing for time tag errors are described under the data processing section. This section is only meant to order the importance of the errors and consider their effect on the range rate measurement error. If range rate measurement errors for frequency $(f_b + f_d)$ and time interval δ_{RR} are greatly reduced, then time tag errors will require similar reductions. At present, the uncertainty in the WWV transmission time is the greatest unknown source of error in time tagging.

4.0 THE RANGE MEASUREMENT

The range measurement in a measure of the time interval between the transmission of a time marker or reference and the reception of that time marker returned from the cooperative target. The time marker in the case of the GRARR system is a mark or reference on the phase of the ground oscillator, f_t. Upon reception of that phase marking the intervening time interval is measured and represents the time delay for the reference mark to travel to and from the cooperative target. Given a constant velocity, c, for the travel of the reference mark to and from the target, then:

$$2R = c\,\delta_R \tag{23}$$

where R is range in meters, c is the constant speed of light in meters per second, and δ_R is the time interval in seconds.*

Within the cooperative target the phase mark on f_t in the uplink is transferred to a phase mark on the spacecraft frequency Nf_0 in the downlink. Associated with this action performed on the spacecraft is a delay which prevents the turnaround of the phase marking from occurring in zero time.

4.1 TRANSPONDER DELAY

The required selectivity built into the spacecraft transponder imposes a delay on the passage of the time reference mark through the transponder. Variations of input frequency to the transponder caused by the Doppler shift impose time delay variation of the time reference mark through the transponder. For a discussion of these points, see Reference 12. Hence Equation 23 must be modified to account for the time delay through the transponder, a function of the Doppler shifted uplink frequency, Kf_t:

$$2R = c\left\{\delta_R - \Delta\tau\left[f\left(Kf_t\right)\right]\right\} \tag{24}$$

*No attempt is made here to consider the bending of the path of travel in the earth's atmosphere, which makes the line of sight distance shorter than R, the measured distance.

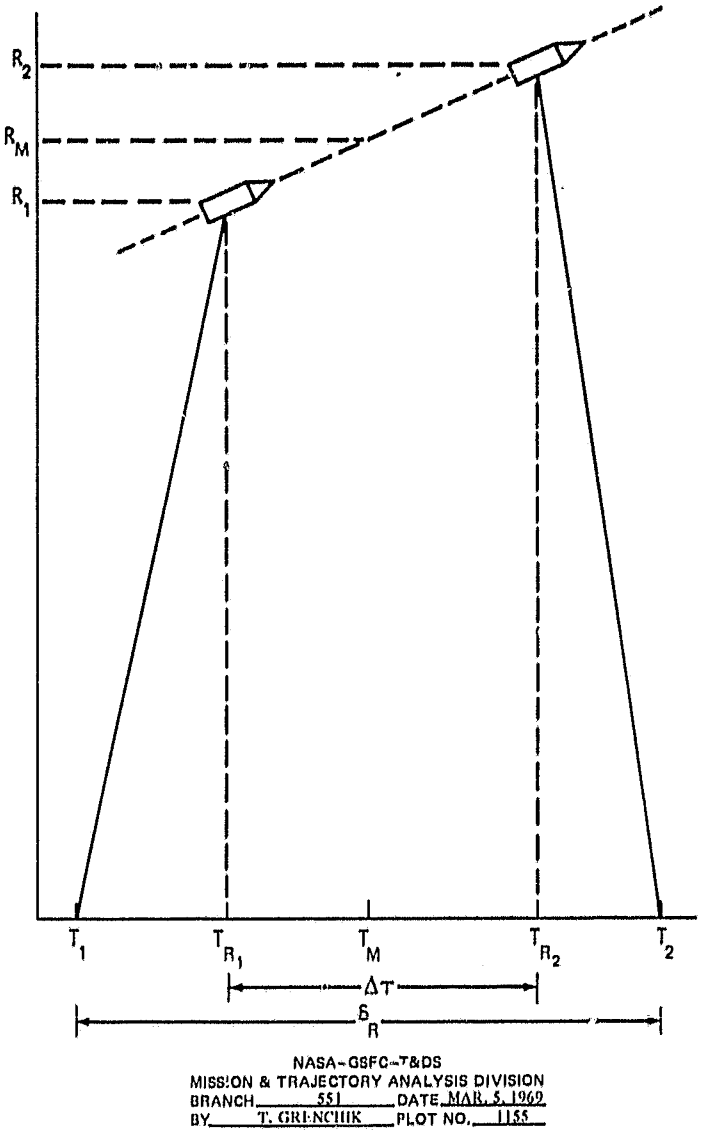

Figure 4—Range measurement.

where $\Delta\tau$ is the time delay of the time reference mark through the transponder. For exactness however, Equation 24, should contain additional terms. These terms have been neglected as insignificant, but it is of interest to examine their magnitudes.

Figure 4 shows the important events in the range measurement sequence. δ_R, the time interval measurement of the system is:

$$\delta_R = \left(T_{R_1} - T_1\right) + \Delta\tau + \left(T_2 - T_{R_2}\right) \tag{25}$$

$$\delta_R = \frac{R_1 + R_2}{c} + \Delta\tau \tag{26}$$

A simplification has been made by omitting the ambiguities in the measurement. This will be defined and covered in a later section. Just as for the range rate measurement, the change in range from the beginning to the end of the transponder delay should be considered to determine its effect upon the measurement. R_1 and R_2 can be expressed in terms of R_M and T_M by a Taylor series expansion of R in the neighborhood of the point $t = T_M$

$$R(t) = R(T_M) + \frac{dR}{dt}(T_M)\left[t - T_M\right] + \frac{1}{2}\frac{d^2 R}{dt^2}(T_M)\left[t - T_M\right]^2 + \cdots \tag{27}$$

Use of Equation 27 for the purpose here is approximate for 2 reasons, one, that by truncating the series with a finite number of terms one neglects the contribution of higher order derivatives of R, and two, considering the neighborhood of the point T_M to include the transponder delay $\Delta\tau$ is not completely rigorous. In defense of the approximation in Equation 27, because of orbit dynamics it is very unlikely that a large number of higher order derivatives of R are significant over a short period of time. Secondly, the transponder delay, $\Delta\tau$, is never larger than 18μ seconds.

To evaluate Equation 27 for $R = R_1$ and $R = R_2$, insert the appropriate values for the time and range values into Equation 27

$$R_1 = R(T_M) + \frac{dR}{dt}(T_M)\left[T_1 - T_M\right] + \frac{1}{2}\frac{d^2 R}{dt^2}(T_M)\left[T_1 - T_M\right]^2 + \cdots \tag{28a}$$

$$R_2 = R(T_M) + \frac{dR}{dt}(T_M)\left[T_2 - T_M\right] + \frac{1}{2}\frac{d^2R}{dt^2}(T_M)\left[T_2 - T_M\right]^2 + \cdots \tag{28b}$$

But

$$T_1 - T_M = -\frac{\Delta\tau}{2} \tag{29a}$$

and

$$T_2 - T_M = \frac{\Delta\tau}{2} \tag{29b}$$

so that

$$R_1 + R_2 = 2R(T_M) + \frac{d^2R}{dt^2}(T_M)\left(\frac{\Delta\tau}{2}\right)^2 + \cdots \tag{30}$$

and all terms except even order derivatives drop out because of the difference in sign on $\Delta\tau/2$. The assumed worst case value of d^2R/dt^2 is 435 meters per second squared. Using this value for the second term in Equation 30, one obtains:

$$\left[\frac{d^2R}{dt^2}(T_M)\left(\frac{\Delta\tau}{2}\right)^2\right]_{\text{MAX VALUE}} = 3.5\,(10^{-8})\text{ meters} \tag{31}$$

It is readily agreed that this value is negligible when compared to the system accuracy requirements. Thus Equation 26 becomes:

$$\delta_R = \frac{2R(T_M)}{c} + \Delta\tau \tag{32}$$

4.2 TABULATION OF RANGE MEASUREMENT ERRORS

References 2, 3, and 4 consider the effects of various errors in the range measurement and place magnitudes on their measurement errors. Here as in the range rate description the intent is to catalog the errors according to source. For range the three classes of error are:

- All sources that cause phase (frequency) errors in the phase marking of f_t and Nf_0.
- All sources that cause time interval measurement errors for δ_R.
- All sources that cause error in identifying the correct time of the sample measurement.

The first two sources of error are adequately covered in References 2, 3, and 4 and no further discussion will be given here. The 3rd source will be considered further.

5.0 DISCUSSION OF TIME TAG ERRORS IN RANGE MEASUREMENT

Figure 5 illustrates the significant times and time intervals for the range measurement. Reference 8 describes the method used in removing equipment delay times in the measurement of δ_R, but Reference 8 does not describe how this "zero set" of range affects the range data time tagging. Figure 5 attempts to show the displacement of the measurement from the time tag. Definitions are as follows:

T_D - Data time as reported for range measurement in GRARR format.

ΔT_F - Delay caused by filtering of phase marking tones after generation in time code generator.

ΔT_R - Time interval following $T_D + \Delta T_F$, after which range measurement actually starts.

ΔE_{R_1} - Time delay from origination point of phase marking to transmission from antenna.

ΔT - Time interval for range to and from collimation tower (used in zero set) to system antennas.

δ_R - System measurement time for zero set procedures (precalculated).

ΔE_{R_2} - Time delay from reception of spacecraft signal at ground antenna to completion of range measurement, δ_R.

Reference 5 describes the mechanization of the phase marking procedure. In the GRARR Motorola system low frequency tones, 8 Hz, 32 Hz, 160 Hz, 800 Hz, 4000 Hz, 20,000 Hz, and 500,000 Hz, are used to phase mark the transmit frequency.* The generation of these tones in the GRARR time code generator results in square wave signals which require filtering to remove the undesired higher harmonics. It is this filter delay which is described as ΔT_F. The phase marking tones in square wave form are in synchronization with the data time T_D since they are all generated in the same circuitry, the GRARR time code generator. After filtering the sinusoidal phase marking tones are delayed with respect to T_D.

ΔT_R is a delay incurred in the start pulse generator which produces the signal to begin the δ_R measurement. The delay, ΔT_R, is 25, 30, or 31μ seconds, depending upon whether the 500 kHz, 100 kHz, or 20 kHz is the highest frequency used in modulating (reference marking) the uplink frequency, f_t.

ΔE_{R_1} and ΔE_{R_2} are all other delays occurring in the system between the equipment and the antennas. How these delays, and the others mentioned above, affect the time tagging will be explained

*A current modification program will also allow modulation with a psuedo random code for ambiguity resolution.

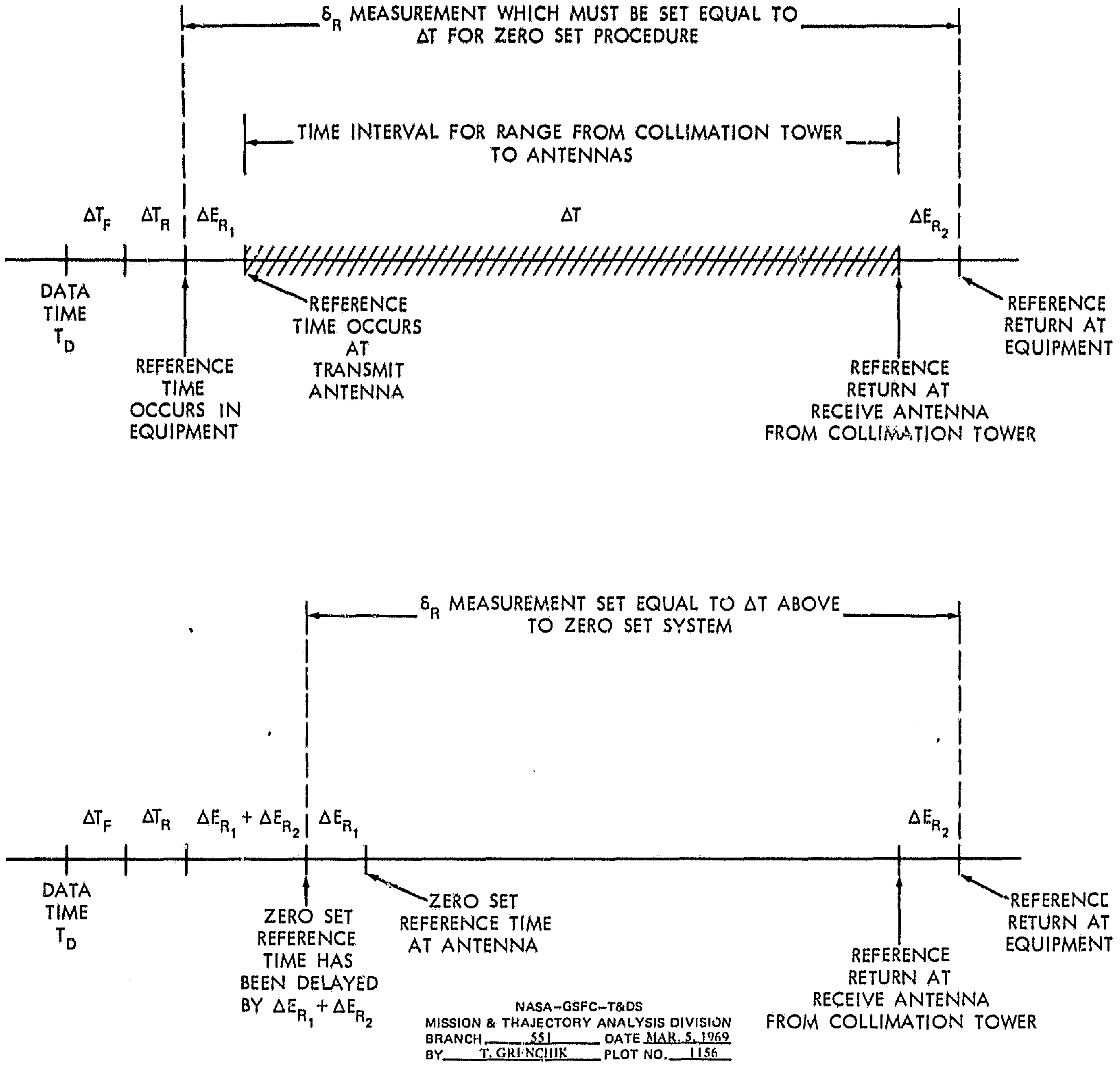

Figure 5—Displacement of reference time from reference time with zero-set procedure.

by reference to Figure 5. If the method of GRARR system zero-set is understood, the time tag errors are readily apparent. The measurement desired, δ_R, is the 2 way travel from transmit antenna to target and back to the receive antenna. (Recall that the Y axis of the receive antenna in the reference point of the system.)

In the top figure of Figure 5, the data time T_D occurs, and some time later after ΔT_F and ΔT_R, the reference time is reached. This is the time at which the measurement δ_R begins. Some time later (after ΔE_{R_1}) the reference marked transmission leaves the transmit antenna, is turned around by a target on a collimation tower, and is returned to the receive antenna. This 2 way distance to the collimation tower (used in zero setting) is known very accurately by survey measurement. The returned transmission then passes through the equipment, (delay time ΔE_{R_2}) and completes the δ_R measurement.

In the lower figure of Figure 5, the δ_R measurement which includes ΔE_{R_1} and ΔE_{R_2} must be set equal to the accurately determined 2 way delay to the collimation tower in order to zero set the system. This is done as follows: The data time T_D and the reference return at the equipment are fixed and unchangable. The only adjustment that can be made is adjustment of the reference time within the system. This is delayed a time, $\Delta E_{R_1} + \Delta E_{R_2}$, so that the adjusted δ_R measurement now agrees exactly with the survey measurement to and from the collimation tower.

It follows then that the time tag for the range measurement (spacecraft time) should be:

$$T_R = T_D + \Delta T_F + \Delta T_R + \Delta E_{R_1} + \Delta E_{R_2} + \frac{\delta_R}{2} \quad (33)$$

Ambiguity terms have been omitted for clarity. Equation 33 requires adjustment of station data time T_D to WWV time just as described under time tagging for the range rate measurement

$$T_R = T_L + WWV + \Delta T_F + \Delta T_R + \Delta E_{R_1} + \Delta E_{R_2} + \frac{\delta_R}{2} \quad (34)$$

Except for the term ΔT_R, the proven magnitudes of ΔT_F, ΔE_{R_1}, and ΔE_{R_2} are unknown at this time. In Reference 9, a delay of 2.1 milliseconds was attributed to a time tag error in the GRARR system at Rosman, North Carolina. Verification of the time delays, ΔT_F, ΔE_{R_1}, and ΔE_{R_2} remain for future work.

A review of the time tag errors for the range measurement show the order of importance for the errors to be as follows:

	Maximum Error in Time Tag	Maximum Range Error ($dR/dt = 10^4$ m/sec)
• $\delta_R/2$, if not considered in data processing	1,250,000μ sec (one-way delay to moon)	12,500 m
• $\Delta T_F + \Delta T_R + \Delta E_{R_1} + \Delta E_{R_2}$, if not considered in data processing	2000μ* sec	20 m
• WWV uncertainty	100-1000μ sec	1-10 m

In the case of range, it appears that the WWV uncertainty is not the predominant error in the time tagging. Further effort will be expended in field measurement of the system delays.

*Value of time tag error taken to be equal to Roman bias (Reference 9).

6.0 PREPROCESSING OF RANGE, RANGE RATE, AND ANGLE TRACKING DATA

6.1 INTRODUCTION

Up to this point the discussion has been restricted to the field station measurement or the acquisition of the raw (uncorrected) range, range rate, and angle tracking data. In this portion of the document the viewpoint will be slanted toward the preprocessing of this raw data prior to its use in orbit computation. The process described herein includes the raw data reading, raw data smoothing, and conversion from range and range rate data in time intervals (seconds) to range and range rate values in meters and meters per second. The preprocessing methods do not include corrections for refraction.

6.2 GENERAL DESCRIPTION AND PURPOSE OF PREPROCESSING

The preprocessing program performs the following general functions.

- It smooths by least squares fit to selectable order (up to 6th degree) Chebyshev polynomials large (up to 400 points) groups of raw data. The purpose of this large scale smoothing is to identify "bad" data points and to provide an estimate of data scatter (standard error of fit). Bad data points are identified by rejecting data points whose residuals exceed some factor of the standard error of fit. Iteration and rejection is continued until the percent change in the standard error reaches some specified number.

- It computes processed data points for orbit determination using the following techniques: from the large groups of data smoothed, small groups of data points are selected. A single point is computed from the fitting polynomial at the center of the small group. These points are then converted to output (processed) points as described in the succeeding sections of this report.

6.3 POLYNOMIAL FITTING TO RAW DATA

The raw data measurements, in units of μsec, are functions of time and are fit to polynomial expansions in time. A least squares solution using Chebyshev polynomials is performed on blocks of data points (nominally 96).

6.3.1 Least Squares Solution

Given is a set of $N + 1$ discrete data points $\{f(x_0), \cdots, f(x_n)\}$. The approximating function $y(x)$ which approximates (fits) these data points is

$$f(x) \approx \sum_{k=0}^{n} a_k \phi_k(x) \equiv y(x)$$

where $\phi_0(x), \cdots, \phi_n(x)$ are $n + 1$ appropriately chosen functions. Define the residual $R(x)$

$$R(x) = f(x) - \sum_{k=0}^{n} a_k \phi_k(x) = f(x) - y(x)$$

and the least squares property is defined as

$$\sum_{\ell=0}^{N} R(x_\ell)^2 = \sum_{\ell=0}^{N} \left[f(x_\ell) - \sum_{k=0}^{n} a_k \phi_k(x_\ell) \right]^2 = \text{minimum} ,$$

This is equivalent to saying

$$\frac{\partial}{\partial a_r} \left(\sum_{\ell=0}^{N} \left[f(x_\ell) - \sum_{k=0}^{n} a_k \phi_k(x_\ell) \right] \right)^2 = 0$$

for $r = 0, \cdots, n$

or
$$\sum_{\ell=0}^{N} \phi_r(x_\ell) \left[f(x_\ell) - \sum_{k=0}^{n} a_k \phi_k(x_\ell) \right] = 0$$

for $r = 0, \cdots, n$

or
$$\sum_{k=0}^{n} a_k \sum_{\ell=0}^{N} \phi_r(x_\ell) \phi_k(x_\ell) = \sum_{\ell=0}^{N} \phi_r(x_\ell) f(x_\ell)$$

for $r = 0, \cdots, n$. The final equation describes $n + 1$ simultaneous equations in the $n + 1$ unknown parameters $a_0, a_1, \cdots, a_n$. These equations are called the normal equations of the process. (See Ch. 7, Reference 14, Hildebrand.)

Written in matrix notation we have $D\hat{E} = F$ and D is a square symmetric matrix with the general element

$$d_{st} = \sum_{\ell=0}^{N} \phi_s(x_\ell) \phi_t(x_\ell)$$

$s, t = 0, \cdots, n$ and F is a column vector with

$$f_s = \sum_{\ell=0}^{N} \phi_s(x_\ell) f(x_\ell)$$

$s = 0, 1, \cdots, n$. Vector $\hat{E}$ is the solution. $(\hat{E} = D^{-1} F)$. (See Reference 15, Berztiss.)

6.3.2 Choice of Chebyshev Polynomials as the Data Approximating Function

Most often it is asked "Why not use the monomials (Taylor series expansion about $x = 0$)?" That is, let $\phi_0(x) = 1$,

$$\phi_1(x) = x, \cdots, \phi_n(x) = x^n$$

and

$$f(x) = a_0 + a_1 x + \cdots + a_n x^n .$$

As described in the referenced Berztiss paper, the matrix D in the case of the monomial expansion has a much greater tendency to be badly ill-conditioned than an expansion in terms of orthogonal polynomials.

So one turns to orthogonal polynomials, which are defined as satisfying the condition

$$\int_a^b \phi_i(x)\phi_k(x)\,dx = 0 ,$$

for the set of functions $\phi_0(x), \cdots, \phi_n(x)$, over the range $a \le x \le b$. The Chebyshev polynomials, $T_i(x)$, have the orthogonality property

$$\int_{-1}^{1} \frac{T_r(x)\,T_s(x)}{\sqrt{1-x^2}}\,dx = 0 \qquad (r \neq s)$$

which makes them orthogonal with respect to the weight factor $1/\sqrt{1-x^2}$.

In the special case when $x_1, \cdots, x_N$ are the N zeros of $T_n(x)$, the off diagonal terms of the matrix D vanish and the Chebyshev polynomials are truly orthogonal. It is a desirable property of orthogonal polynomials, that the D matrix becomes a diagonal matrix. Although the zeros of the $T_n(x)$ polynomial are never available, the resulting D matrix from the Chebyshev polynomial solution has comparatively small off diagonal terms and makes the solution well defined. According to Berztiss, Reference 15, the use of Chebyshev polynomials compared to monomials improved the accuracy for a 10th degree polynomial by approximately four significant figures using a single precision arithmetic in a computer. This difference between the Chebyshev and the monomial accuracy could have been made arbitrarily small if arithmetic of sufficiently high precision (i.e. double precision) had been used, but it does illustrate the advantages of minimizing the values of the off diagonal terms in the D matrix.

The Chebyshev polynomials used in the preprocessing are:

$$y(x) = \sum_{k=0}^{n} a_k T_i (x)$$

where

x = time normalized to [-1, 1] interval

a_k = the desired coefficcients

n = the degree of the polynomial

$T_i (x)$ = the Chebyshev polynomials

where

$$T_0 (x) = 1$$

$$T_1 (x) = x$$

$$\vdots$$

and

$$T_{r+1} (x) = 2x T_r (x) - T_{r-1} (x)$$

6.4 ORB 1 TAPE

Some of the difficulties inherent in the preprocessing of raw data stem from insufficient data available from raw data sent from the field stations. For example the reported range measurement may be ambiguous in that from the data message one cannot determine if the range is 18,750 kilometers or multiplies of 18,750 kilometers. This difficulty is circumvented by the prior preparation of an ORB 1 tape, which is used in conjunction with the data preprocessing. The ORB 1 tape is a record which contains an ephemeris of position and velocity of a satellite with reference to the center of the earth.

There are several Orbit Generator Routines in the final orbit determination program that have as a by-product an ORB 1 tape. The Cowell Integration Orbit Generator Routine is the most frequently used at the present time. Needed as input to these routines is a set of orbital elements (coordinates that can be converted to position and velocity at that time) and a time to be associated with this set of elements. When a satellite is first launched, the elements used to create the first ORB 1 tape, are the predicted elements. When the first data comes in, it is in conjunction with these initial elements that the observations are differentially corrected in the final orbit determination program and a new set of orbital elements are computed. With this new set of elements a new ORB 1 tape can be generated. For most satellites, after a satellite's orbit has been fairly well determined, it is necessary to update the orbit about once a week. Regardless of the means of preparation, it is this ORB 1 tape which is used in raw data preprocessing. Its specific usage in preprocessing will become more evident in later sections of this report.

6.5 RANGE MEASUREMENT DESCRIPTION

The GRARR range measurement is a count of a reference frequency (100 MHz) from a start time (signal transmission) until a stop time (signal reception). Knowing the reference frequency this count can easily be converted into a time interval measurement. Using the speed of light one can convert the time interval measurement into a distance measurement.

6.5.1 Raw Data Format

The preprocessing program accepts the raw data in the formats governed by the Stadan Engineering Division, Code 570. A description of the data formats is best available in a GSFC X Document to be published in April 1969, entitled, "DATA FORMATS OF THE GODDARD RANGE AND RANGE RATE SYSTEM AND THE APPLICATIONS TECHNOLOGY SATELLITE RANGE AND RANGE RATE SYSTEM," by DAVID ZILLIG, Code 571.

6.5.2 Range Measurement Ambiguity*

The time interval counter for the range measurement has a maximum value which is determined by the lowest frequency sidetone (usually 8 Hz). The 100 megahertz counter is started on an even increment of time (usually once per second). The event that stops the counter is the return of a positive going zero crossing of the 8 Hz modulating waveform upon return from the target. The time interval between two cycles of the 8 Hz sinusoid is .125 seconds.

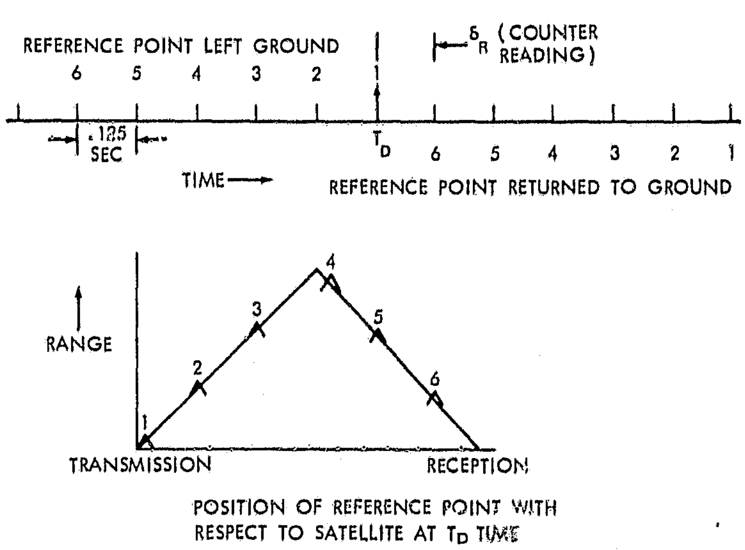

Figure 6—Ambiguity illustrations.

If a satellite's range requires more than .125 seconds for the wave to be transmitted and received (a range of about 18,500 km) we say it is out of the first range gate and depending on which range gate it is in, a fixed quantity of time must be added to the measurement.

To illustrate, let a time mark (8 Hz positive going zero crossing) be sent at T_D where T_D is the time associated with the raw data. Figure 6 illustrates how ambiguity occurs. Let $\wedge$ indicate the positions of positive going zero crossings of the 8 Hz modulation on the transmitted carrier wave as the range measurement is occurring. The event that stops the range time interval counter is the reception of number "6" positive going zero crossing. Number "1" 8 Hz positive going zero crossing is beginning transmission at T_D. The time measured δ_R is the time required for number 6 to complete its trip.

*The ATSR system requires ambiguity resolution. In the near future all GRARR systems will have self-contained ambiguity resolution.

Therefore, the desired transmitted time is when number "6" left the ground and to compute the proper range the number of gates or ambiguities must be added to the computed range. For this example it would be necessary to add .625 seconds (5 × .125) to the range time interval counter reading.

6.5.3 Conversion of Range to Metric Quantity

Let δ_R be the two way delay time (range measurement) in seconds, $\Delta\tau$ be the transponder delay and c is the speed of light. From distance equals velocity multiplied by time one obtains:

$$\text{range} = R = \frac{c}{2}\left(\delta_R - \Delta\tau\right)$$

If an ambiguity is present, this equation must be modified to:

$$R = \frac{c}{2}\left(\delta_R - \Delta\tau + N_A \Delta A\right)$$

where

$\Delta\tau$ = transponder delay

N_A = the ambiguity number

ΔA = size of the ambiguity interval in time

δ_R = two way delay time

To determine N_A use the ORB 1 tape described previously to compute range at T_D where T_D is the data time. Let

R_C = range computed from ORB 1 tape

$R_1 = \frac{c}{2}\,\delta_R$, range computed from measurement ignoring ambiguity

R_A = the range associated with ΔA time (gate size)

Then let N_A be the integer closest to X_A when,

$$X_A R_A = R_c - R_1 \quad \text{or}$$

$$X_A = \frac{R_c - R_1}{R_A}$$

6.5.4 Range Measurement Time Tagging

The data comes in tagged with a raw data time T_D. To associate the proper data time with the measurement it is necessary to know the approximate orbit. The ORB 1 tape is used for this purpose. From the ORB 1 tape, which contains an ephemeris of geocentric position and velocity, a theoretical range with respect to a particular station can be computed. The desired time to be associated with the theoretical range is satellite time, that is the time of the range measurement at the satellite and not the time at the ground station. The data however, is time tagged at the ground, introducing errors because of the time required for the signal to reach the ground, the time required for the signal to go through the transponder, (transponder delay), the WWV time delay (defined earlier) as well as ground equipment delays.

In order to determine the midpoint time of the entire measuring interval (from the time the signal leaves the ground to the time it is received) we use the ORB 1 tape to determine the approximate range. The transmitted signal time is unknown. The received signal time can be computed using the raw data tag, the measurement and the WWV correction. From the ORB 1 tape, the approximate range at the received time can then be computed. Since $R = ct$ and $t = R/c$, the midpoint time can be estimated, and the approximate range at the midpoint can be recomputed. This value is used to compute the midpoint time. The time is then corrected for the transponder delay.

Let

T_D = raw data time

R = the time measurement

N_A = the ambiguity number

ΔA = the size of the ambiguity in time

T_R = the proper data time tag

WWV = WWV delay

c = speed of light

$R_c(t)$ = range computed from the ORB 1 tape at time t.

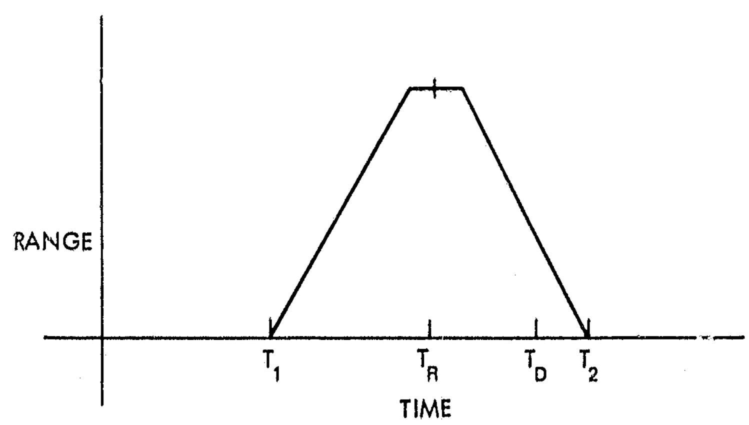

$$T_2 = T_D + \delta_R + WWV \qquad T_{2,s_1} = T_2 - \frac{1}{c} R_c(T)$$

As a first approximation use T_2 as an estimate for satellite time to compute R_c at T_R.

As a second approximation

$$T_{2,s_2} = T_2 - \frac{1}{c} R_i\left(T_{2,s_1}\right)$$

This is sufficiently accurate at this time, and all that is necessary is to subtract for the transponder delay of the satellite. The transponder delay is a function of the range rate of the satellite.

Let $\Delta\tau\,(dR(t)/dt)$ be the transponder delay as a function of range rate dR/dt computed from the ORB 1 tape at time t.

Then

$$T_R = T_{2,s_2} - \frac{1}{2}\Delta\tau\left[\frac{dR}{dt}\left(T_{2,s_2}\right)\right]$$

is the time tag to be associated with the range measurement.

6.6 RANGE RATE MEASUREMENT DESCRIPTION

The range rate measurement is a count of a reference frequency (10 MHz)* starting with the first of N cycles of $f_b + f_d$ (bias + doppler frequencies) and stopping upon the completion of the N^{th} cycle. By knowing the reference frequency, one can interpret the measurement as a time interval measurement, a time interval required to count to a known value N of cycles of doppler and bias frequency.

6.6.1 Range Rate Formula Derivation and Averaging Effect Correction

Let δ_{RR} be the time it takes to measure N cycles of doppler frequency, f_d, plus bias frequency, f_b, in the range rate counter.

$$N = \left(f_d + f_b\right)\delta_{RR}$$

Since the measuring over N cycles takes a finite amount of time, the measurement is an average range difference. It is necessary to make a correction to the average range difference, using the ORB 1 tape, in order to make the measurement an instantaneous range difference. This is necessary since the orbit determination requires an instantaneous measurement.

Let

$\Delta R\left(\delta_{RR}\right)$ = the change in range during the ground time interval δ_{RR}

c = the speed of light

f_t = the uplink frequency

f_d = the 2 way doppler frequency

f_b = the bias frequency

*For ATSR range rate, the reference frequency is 100 MHz.

$$\Delta R(\delta_{RR}) = \frac{-c}{f_t}\left(\frac{f_d}{2}\,\delta_{RR}\right)$$

which is the wave length of the transmitted signal multiplied by the average two way doppler frequency divided by 2, multiplied by the measurement time. The negative sign if necessary to maintain the convention of negative doppler frequency corresponding to a positive change in range.

Since

$$N = (f_d + f_b)\,\delta_{RR}\,, \qquad f_d\,\delta_{RR} = N - f_b\,\delta_{RR}$$

and $\Delta R(\delta_{RR})$ becomes

$$\Delta R(\delta_{RR}) = \frac{-c}{2f_t}\left(N - f_b\,\delta_{RR}\right)$$

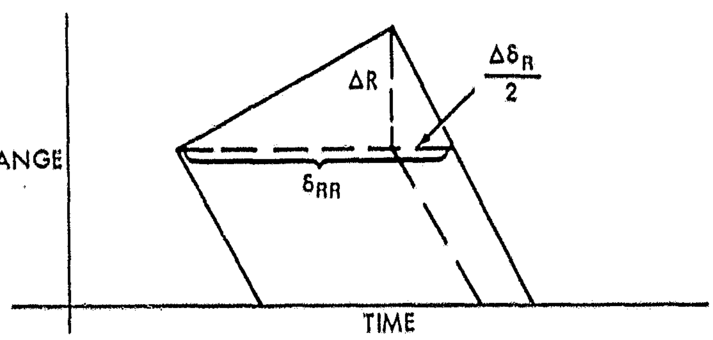

The time to be associated with this change in range needs to be satellite time.

$$\Delta R = \frac{c}{2}\,\Delta\delta_R$$

$$\frac{\Delta R}{c} = \frac{\Delta\delta_R}{2}$$

where $\Delta\delta_R$ is the change in two way delay time due to the change in range. Then for satellite time

$$\Delta t = \delta_{RR} - \frac{\Delta\delta_R}{2}$$

$$\Delta t = \delta_{RR} - \frac{\Delta R(\Delta t)}{c}$$

$$= \delta_{RR} + \frac{1}{2f_t}\left(N - f_b\,\delta_{RR}\right)$$

since Δt at the satellite corresponds to δ_{RR} on the ground. Then:

$$\frac{\Delta R(\Delta t)}{\Delta t} = \frac{\frac{-c}{2f_t}\left(N - f_b\,\delta_{RR}\right)}{\delta_{RR} + \frac{1}{2f_t}\left(N - f_b\,\delta_{RR}\right)}$$

which is the average range difference for that time interval.

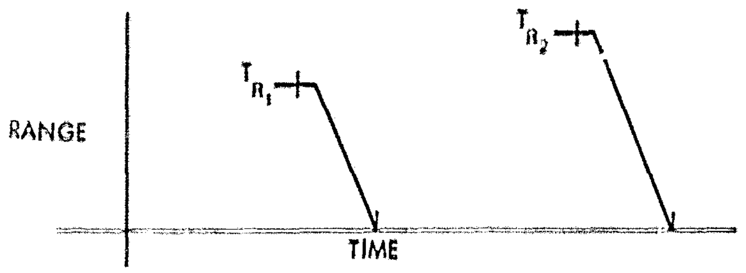

To correct for the fact that this is an average range difference the ORB 1 tape is used. Theoretical ranges are computed at T_{R_1} (R_1), and at T_{R_2} (R_2), and the theoretical range rate dR/dt at $(T_{R_1} + T_{R_2})/2$.

The correction is then

$$\text{corr} = \frac{dR}{dt} - \left(\frac{R_2 - R_1}{T_{R_2} - T_{R_1}}\right)$$

and

$$\frac{dR}{dt} = \frac{\Delta R(\Delta t)}{\Delta t} + \text{corr}$$

is the corrected instantaneous range rate.

6.6.2 Range Rate Time Tagging

The time associated with the range rate measurement is a reference time that needs to be adjusted to satellite time. In essence the midpoint of the measuring interval is to be computed. Since the satellite is moving during the ground station measurement of the N cycles of $f_b + f_d$, it is necessary to determine where the satellite was at two points, the beginning and the end of the measuring interval. At these two points it is necessary to determine the satellite time. The procedure is the same as for the range measurement but two points in time are needed for the range rate measurement.

Let

T_D = raw data time

δ_{RR} = the time measurement

T_{RR} = the proper data time tag

WWV = WWV delay

c = speed of light

$R_c(t)$, $dR(t)/dt$ = range, range rate computed from the ORB 1 tape at time t.

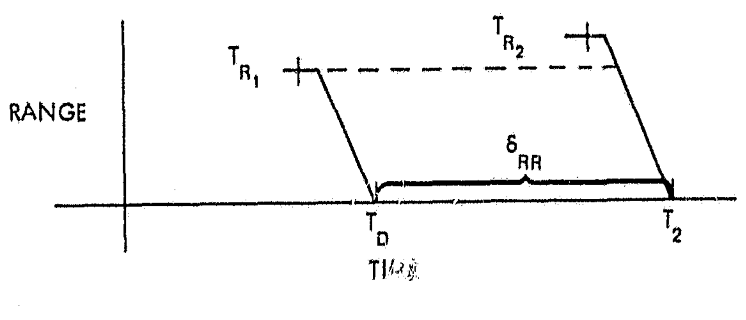

$$T_2 = T_D + \delta_{RR} + \text{WWV}$$

Using the same procedure as used in the range computation and letting

$$T_{R_2} = T_{2,s_2} - \frac{1}{2}\Delta\tau\left(\frac{dR}{dt}\left(T_{2,s_2}\right)\right)$$

Substituting T_D for T_2

$$T_{R_1} = T_{D.s_2} - \frac{1}{2}\,\tau\left(\frac{dR}{dt}\left(T_{D.s_2}\right)\right)$$

Then

$$T_{RR} = \frac{T_{R_1} + T_{R_2}}{2}$$

Note that minor delays through the equipment are ignored.

6.7 DATA OUTPUT FOR THE DIFFERENTIAL CORRECTION PROGRAM

The actual procedure used to obtain representative points for the Differential Correction Program (final orbit determination) is as follows:

- Smooth the raw data as a function of raw data time (equally spaced intervals) and obtain coefficients for the representative Chebyshev polynomials. Use all the data points and obtain a fit. Reject data points outside a predetermined number of sigma, (root mean square of the residuals) away from the curve. Compute new coefficients and continue in this process until sigma remains relatively constant or no new points are thrown out.
- Choose output times and compute corresponding measurements from the polynomials.
- Convert to range and range rate measurements.
- Make time corrections.

7.0 CONCLUSION

It has been the purpose of this paper to shed some light on the range and range rate measurements and how they are processed prior to orbit computation. In particular, most errors of the system are tabulated and ranked. When correction is warranted, a method of correction is indicated. It is the hope of the authors that this description and partial analysis will prove useful to persons interested in the GRARR and ATSR tracking systems.

Acknowledgment and thanks is made for the helpful suggestions in formula derivations and time corrections to Dr. Joseph Siry and Mr. David Stewart.

REFERENCES

1. *The Goddard Range and Range Rate Tracking System: Concept, Design and Performance.* By G. C. Kronmiller, Jr. and E. J. Baghdady, Report X-531-65-403, Goddard Space Flight Center, October 1965.

2. *Goddard Range and Range Rate System Design Evaluation Report,* Motorola Inc., Military Electronics Division, Phoenix, Arizona, Motorola Report No. W 2719-2-1, 23 November 1962.

3. *Design Evaluation Report for Goddard Range and Range Rate System (GRR-2),* General Electric Company, Military Communications Department, Oklahoma City, Oklahoma, November 1964.

4. *Design Evaluation Report Goddard Range and Range Rate System,* General Dynamics Electronics Division, San Diego, California, General Dynamics Report No. R-67-042, 13 December 1967.

5. *Handbook Goddard Range and Range Rate System,* Motorola Inc., Military Electronics Division, Phoenix, Arizona, Motorola No. MH - 1016, 1 July 1964.

6. *The Doppler Equation In Range and Range Rate Measurement,* by B. Kruger, Report X-507-65-385, Goddard Space Flight Center, 8 October 1965.

7. *The Range Rate Error Due to the Averaging Techniques of Doppler Measurements,* By B. Kruger, Report X-513-65-100, Goddard Space Flight Center, 5 March 1965.

8. *NASA-GSFC GRARR Zero-Set Numbers,* Prepared by Tracking Section, Network Engineering Branch, Code 571, Goddard Space Flight Center, February 1968.

9. *Intercomparison of Collocated Laser Optical and GRARR Radio Ranging System Tracks on GEOS-4,* By John H. Berbert, Et Al, Report X-514-67-447, Goddard Space Flight Center, September 1967.

10. *Theory of Phase Lock Techniques,* By Floyd M. Gardner, Et Al, Resdel Engineering Corporation, Pasadena, California.

11. *NBS Standard Frequency and Time Services,* Miscellaneous Publication 236, 1966 Edition, Prepared by U.S. Department of Commerce and National Bureau of Standards.

12. *High Accuracy Satellite Tracking Systems, Special Report,* Adcom, Inc., Cambridge, Massachusetts, 31 May 1963.

13. *Applied Analysis,* by Cornelius Lanzcos, Prentice Hall, Inc.

14. *Introduction to Numerical Analysis,* by F. B. Hildebrand, McGraw-Hill Book Company, Inc. 1956.

15. *Least Squares Fitting of Polynomials to Irregularly Spaced Data,* by A. T. Berztiss, SIAM Review, Vol. 6, No. 3, July 1964, page 203.

Appendix A

Past Preprocessing Methods

A.1 TIME TAG PLACED ON RANGE AND RANGE RATE DATA ON THE IBM 7094 MACHINE

As described earlier in this document, the time tag placed on the raw data at the tracking station is the same for range and range rate measurements, although the time tag should be interpreted differently. The time that this raw data time tag (T_D) represents can be seen from the diagrams.

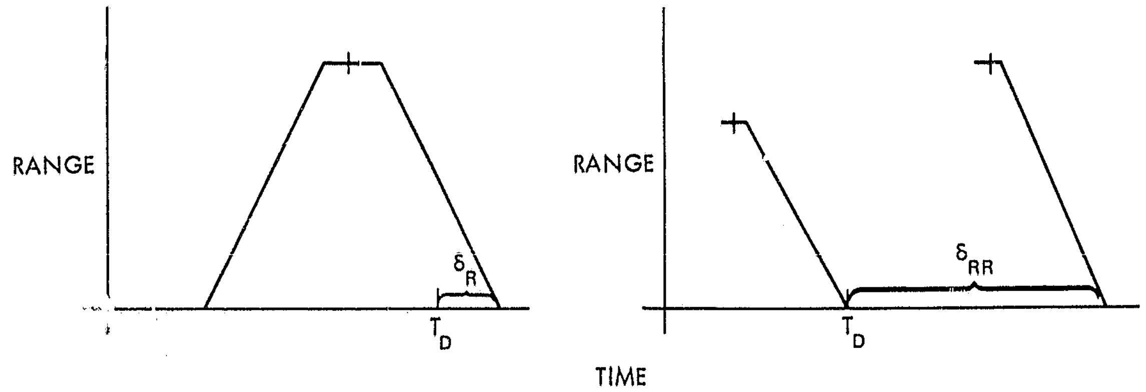

The transponder delay $(\Delta\tau)$ in the IBM 7094 program was taken as a constant. The value chosen was the value at zero doppler frequency. The time tagged to both the range and range rate data by the preprocessor was:

$$T = T_D + WWV + \frac{(\delta_R - \Delta\tau)}{2}$$

expressed in compatible units where WWV is the WWV delay time, and δ_R is the range time measurement. There is an additional time correction applied in the AOPB differential correction program to the range time. When the range ambiguity is resolved the time is adjusted to correspond.

A.2 CORRECTION FOR THE AVERAGING EFFECT ON THE 7094

After the smoothing process, a set of coefficients for the Chebyshev polynomial expressing the range rate measurement (δ_{RR}) as a function of raw data (station) time is available.